jmr&t
Journal of Materials Research and Technology
www.jmrt.com.br

Original Article

TiO_2 nanoparticles immobilized on carbon nanotubes for enhanced visible-light photo-induced activity

Ali Akbar Ashkarran[a,*], *Majid Fakhari*[a], *Habib Hamidinezhad*[b], *Hedayat Haddadi*[c], *Mohammad Reza Nourani*[d]

[a] *Department of Physics, Faculty of Basic Sciences, University of Mazandaran, Babolsar, Iran*
[b] *Department of Basic Sciences, Sari Agricultural Sciences and Natural Resources University, Sari, Iran*
[c] *Department of Chemistry, Faculty of Sciences, Shahrekord University, Shahrekord, Iran*
[d] *Department of Material Engineering, Science and Research Branch, Islamic Azad University, Tehran, Iran*

ARTICLE INFO

Article history:
Received 4 April 2014
Accepted 14 October 2014
Available online 28 November 2014

Keywords:
$CNT–TiO_2$
Nanocomposites
Photocatalysis
Visible-light

ABSTRACT

$CNT–TiO_2$ nanocomposites were prepared through (i) simple mixing of as prepared CNTs and TiO_2 nanoparticles (NPs), (ii) simple mixing of as prepared CNTs and TiO_2 NPs followed by heat treatment and (iii) simple mixing of as prepared CNTs and TiO_2 NPs followed by UV illumination. The synthesis of CNTs and TiO_2 NPs were performed individually by arc discharge in water and sol–gel methods, respectively and characterized by X-ray diffraction (XRD), ultra violet and visible spectroscopy (UV–vis), Fourier transform infrared spectroscopy (FT-IR), scanning electron microscopy (SEM) and transmission electron microscopy (TEM). The visible-light photocatalytic performance of $CNT–TiO_2$ nanocomposites was successfully demonstrated for the degradation of Rhodamine B (Rh. B) as a model dye at room temperature. It is found that $CNT–TiO_2$ nanocomposites extended the light absorption spectrum toward the visible region and considerably improved the photocatalytic efficiency under visible-light irradiation. The visible-light photocatalytic activities of $CNT–TiO_2$ nanocomposites in which CNTs are produced by arc discharge in deionized (DI) water at 40, 60 and 80 A arc currents and combined through three different protocols are also investigated. It was found that samples prepared at 80 A arc current and 5 s arc duration followed by UV illumination revealed best photocatalytic activity compared with the same samples prepared under simple mixing and simple mixing followed by heat treatment. The enhancement in the photocatalytic property of $CNT–TiO_2$ nanocomposites prepared at 80 A arc current followed by UV illumination may be ascribed to the quality of CNTs produced at this current, as was reported before.

* *Corresponding author.*
E-mail: ashkarran@umz.ac.ir (A.A. Ashkarran).
http://dx.doi.org/10.1016/j.jmrt.2014.10.005

1. Introduction

Titanium dioxide has been widely used as an efficient photocatalytic material in decomposing toxic organic molecules to H_2O, CO_2 and other harmless molecules [1,2]. This property also has been applied in inactivation of bacteria and harmful components from water and air, as well as in self-cleaning or self-sterilizing surfaces for places such as medical centers [3–6]. But, the problem is that the band edge of TiO_2 photocatalyst lies in the UV region which covers about 4% of the solar spectrum [7]. Consequently conventional TiO_2 photocatalysts are inactive under visible-light irradiation and as a result with limited practical applications [8]. In this regard, researchers have been interested in the modification of electronic and optical properties of this semiconductor for its efficient use in environmental purification under visible-light irradiation [9,10].

Strategies of making TiO_2 visible-light-active photocatalyst usually classified into three main categories: doping TiO_2 with transition metal ions such as V, Cr, Mn, Fe, Ag, Co, Ni, C; doping nitrogen into TiO_2 and coupling of TiO_2 with a small band-gap semiconductor which extends light absorption into the visible region. Although lots of reports are available on nitrogen and silver doped TiO_2 as two common ways for making visible-light-active photocatalyst but, carbon doped TiO_2 was also as an appropriate alternative among researchers in past years [11,12].

Li and co-workers prepared CNT–TiO_2 nanocomposites using sol–gel method. They have shown that TiO_2 film thickness on the surface of CNTs is the key factor controlling electron transfer and photocatalytic activity in CNT/TiO_2 hybrid nanostructures. It is found that thinner TiO_2 layer enhances photodegradation of methylene blue and higher CNT content in the composites correlates with higher photocurrents and electronic conductivity of the nanocomposites catalyst film increases [13]. Bouazza et al., also synthesized CNT–TiO_2 nanostructures through sol–gel method for the photocatalytic oxidation of propene. They have found CNT–TiO_2 nanocomposites with 70% of TiO_2 and 30% of CNT, shows the highest photocatalytic activity for the oxidation of propene [14].

While most of the reported works for synthesis of visible-light-active TiO_2 were based on sol–gel, hydrothermal or conventional chemical methods [15–23], in this work we introduce a new approach to prepare visible-light-driven TiO_2 photocatalyst using through three different coupling alternatives: (i) simple mixing of as prepared CNTs and TiO_2 nanoparticles (NPs), (ii) simple mixing of as prepared CNTs and TiO_2 NPs followed by heat treatment and (iii) simple mixing of as prepared CNTs and TiO_2 NPs followed by UV illumination.

There are some well defined techniques for synthesis of CNTs, the most common ways of which are chemical vapor deposition (CVD), laser ablation (LA) and electrical arc discharge [24–26]. Among these methods, electrical arc discharge in liquid for production of CNTs attracted much attention because of simplicity of apparatus building, low impurity introduction, no need for complicated vacuum equipment, high-throughput, and cost-effective procedure to generate a high yield of CNTs. The simplicity of this method also allows scaling up for mass production of CNTs [27].

In this study, CNTs and TiO_2 NPs individually were prepared by arc discharge in water and sol–gel methods and then combined through three different coupling alternatives to form CNT–TiO_2 nanocomposites. We have specifically studied the effect of each coupling method on photocatalytic performance of CNT–TiO_2 nanocomposites under visible-light illumination.

2. Experimental details

2.1. *Synthesis of TiO_2 NPs*

For synthesis of TiO_2 NPs 1 mL $TiCl_4$ (Merck, 99%) was slowly added dropwise into 10 mL EtOH (Merck, 99.8%) under vigorous stirring at room temperature. A large amount of HCl gas was exhausted and a transparent yellowish solution was formed. The as prepared solution was dried at 100 °C for 24 h leading to a white amorphous gel. The extracted powder was then annealed at 450 °C for 1 h leading to white crystalline TiO_2 nanopowder.

2.2. *Synthesis of CNTs*

The arc discharge method in DI water was used for synthesis of CNTs. The arc discharge set up includes a high current DC power supply and a reactor including anode, cathode and a micrometer which moves the anode toward the cathode, as we have reported in details in our previous works as a novel technique for synthesis of various nanostructures [27]. In a typical discharge process a 40–80 A current was applied between two graphitic electrodes in DI water. The voltage was dropped to about 10–20 V during the arc formation while the current was fixed to a desired amount. Both the anode and cathode were wire shaped, 2 mm in diameter and 99.9% purity (from Sigma–Aldrich). Initially, we bring the two electrodes into touch leading to a small contact cross section and thus to a high current density. Then we separate them from each other and as a result graphite is ablated from the anode and then condensed in solution and CNTs in addition to some carbonaceous nanostructures are formed.

2.3. *Purification of CNTs*

For purification of CNTs and removing unwanted products such as amorphous carbon, carbon particles and other carbonaceous structures three distinct processes were performed. First, the as prepared solution was dried at 100 °C for 24 h to get a black powder. The powder was then dispersed in ethanol medium and sonicated (using a 30 kHz power for 30 min) for 1 h followed by drying at 60 °C for 12 h and annealing at 500 °C for 1 h. Then, the obtained powder dispersed in 10 mL HCl (Merck, 99%) and sonicated for another 30 min. Finally, all samples centrifuged and washed with DI water followed by drying at 100 °C for 12 h and annealing at 500 °C for 1 h as the last step of purification process.

2.4. Synthesis of CNT–TiO_2 nanocomposites

Three different strategies including simple mixing, UV illumination and heat treatment were performed for coupling of TiO_2 NPs and CNTs. In simple mixing method 0.1 g of TiO_2 powder and 0.02 g purified CNTs were dispersed and mixed in 100 mL DI water under slow stirring rate at room temperature for 15 min. In UV illumination method the suspension prepared by simple mixing method exposed to UV illumination with 254 nm wavelength for 2 h while stirring slowly at room temperature. In the heat treatment method the suspension prepared by simple mixing method dried at 100 °C for 24 h and then annealed at 500 °C for 1 h. This value is the temperature that causes oxidation of amorphous carbon while does not change significantly the anatase crystalline phase of TiO_2 NPs.

2.5. Characterization

Analysis of the crystalline structures was performed by XRD diffractometer (X'pert Philips) equipped with a Philips high intensity ceramic sealed tube (3 kW) X-ray source and wavelength of Cu Kα ($\lambda \sim 1.5405$ Å) radiation in 2θ range from 10° to 90° by 0.005° s^{-1} steps. UV–vis spectroscopy of the samples was taken out by a double beam Optizen POP spectrophotometer (Mecasys Company, Korea) from 200 nm to 1100 nm wavelengths. A Pyris 1 TGA thermogravimetric analyzer was used for the analysis of the composition of CNTs. 1 mg of the sample was heated from 50 °C to 1000 °C with a heating rate of 10 °C min^{-1} under ambient air. FT-IR analysis was performed by a Thermo Nicolet spectrometer equipped with a MCT detector (4 cm^{-1} resolution) and a 100 mW Nd:YAG laser with wavelength of 1064 nm. The spectral resolution was 0.5 cm^{-1}, spot size was 10 mm and precision of wavelength was 0.01 cm^{-1}. SEM analysis was taken out by a SEM instrument (Philips XL30) at 5–20 keV accelerating energy. Before taking images all samples were coated with a 10 nm gold layer using a physical vapor deposition system from Bal-Tec company (Switzerland). TEM analysis was performed by a LEO 912 AB instrument at 150–200 keV accelerating energy by deposition of nanoparticles onto the copper grid at room temperature. DI water was supplied from a Millipore water purification system (Direct-Q-3) with 18.2 MΩ cm (0.055 μs) resistance.

2.6. Photocatalytic activity measurement

Photocatalytic activity of the CNT–TiO_2 nanocomposites was measured by photodegradation of Rh. B as a model dye with the initial concentration and volume of 10^{-5} M and 30 mL respectively at the presence of 30 mL CNT–TiO_2 solution. First the mixed Rh. B and CNT–TiO_2 solution was stirred in dark for 30 min to equilibrate the absorption/desorption between dye molecules and TiO_2 photocatalyst. Then it was irradiated at room temperature by a 90 W halogen lamp. The degradation rate was measured by UV–Vis spectrophotometer at the maximum absorption wavelength of Rh. B.

3. Results and discussion

3.1. XRD analysis of the products

XRD analysis was taken out to find the crystalline phase and structure of the products. The results for pure TiO_2 and CNT–TiO_2 samples are depicted in Fig. 1. XRD results of TiO_2 NPs shows formation of anatase phase peaks at $2\theta = 25.3$, 37.7, 47.8, 54, 62.7 and 75.2 degree with no impurity which is in agreement with 21-1272 standard card from JCPDS [22]. Crystallographic data obtained from XRD demonstrates co-existence of both TiO_2 and CNT in samples prepared by simple mixing and also samples followed by heat treatment or UV illumination. Due to the similar patterns, XRD analysis of

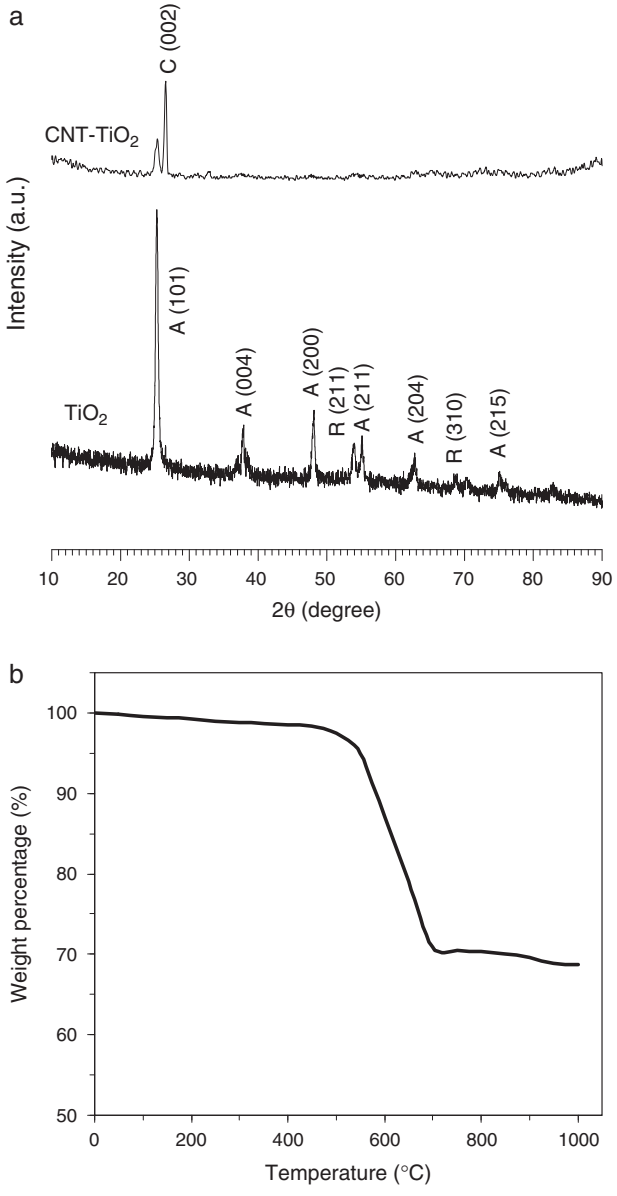

Fig. 1 – Typical XRD patterns of (a) TiO_2 NPs and CNT–TiO_2 nanostructures and (b) typical TGA profile of CNTs (heating was performed at a constant rate of 10 °C min^{-1} in ambient air).

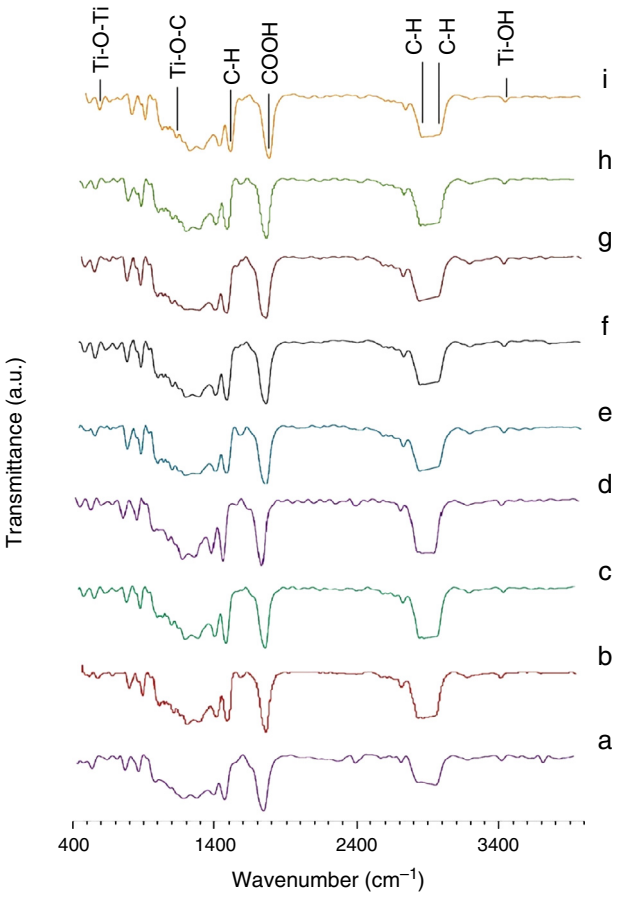

Fig. 2 – FT-IR spectra of CNT–TiO_2 nanocomposites in which CNTs are prepared at 40 A and (a) simple mixed, (b) simple mixed followed by heat treatment, (c) simple mixed followed by UV illumination, CNTs are prepared at 60 A and (d) simple mixed, (e) simple mixed followed by heat treatment, (f) simple mixed followed by UV illumination, CNTs are prepared at 80 A and (g) simple mixed, (h) simple mixed followed by heat treatment and (i) simple mixed followed by UV illumination.

the simple mixed CNT–TiO_2 sample is only demonstrated in Fig. 1b as representative. The peak appeared at $2\theta = 26.95$ is related to formation of (0 0 2) planes of CNTs in which the intensity of TiO_2 peaks somehow decline by mixing CNT with TiO_2 NPs [10]. This is while the main anatase phase peak is still visible at $2\theta = 25.3°$ which is related to (1 0 1) crystalline planes of anatase TiO_2. This calcination temperature was selected both to have a crystallized anatase TiO_2 and avoid from remarkable loss of CNTs from the CNT–TiO_2 structures at higher temperatures (see for example thermal gravimetric analysis (TGA) in Fig. 1c). TGA of pristine CNT showed a negligible mass loss at 500 °C but, above this temperature a progressively increasing rate of mass loss was observed up to the combustion point of 700 °C. Presence of CNTs in TEM images after calcination at 500 °C confirm intactness of the CNTs in this temperature. In fact, between 500 and 700 °C a significant weight loss was observed due to the decomposition of CNTs, as reported by Li and co-workers [13].

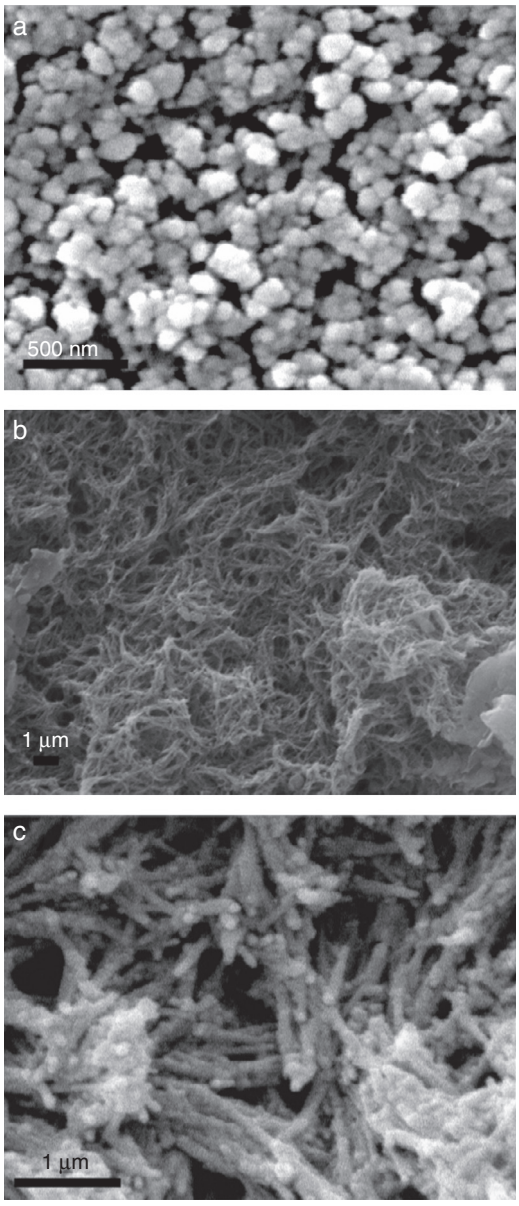

Fig. 3 – SEM images of (a) as prepared TiO_2 NPs, (b) purified CNT prepared through electrical arc discharge in DI water and (c) CNT–TiO_2 NPs coupled via simple mixing method.

3.2. *FT-IR spectroscopy*

Fig. 2 demonstrates FT-IR spectra of CNT–TiO_2 nanocomposites in which CNTs prepared at 40, 60 and 80 A arc currents using arc discharge method and combined through the three mentioned alternatives. The bands at 2847 and 2910 cm^{-1} are assigned to the symmetric and anti-symmetric C—H band related to CH_2 and CH_3 stretching vibrations, respectively. The sharp band of COOH group at 1720 cm^{-1} and 1460 cm^{-1} is related to the anti-symmetric C—H mode of CH_3 bending vibrations due to the presence of CNTs [28,29]. The peaks at 560 cm^{-1} and 1090 cm^{-1} are also attributed to the bending vibrations of Ti—O—Ti and Ti—O—C bonds [30]. In fact, modification of band gap energy of TiO_2 and extension of light absorption into the visible region is due to the presence of

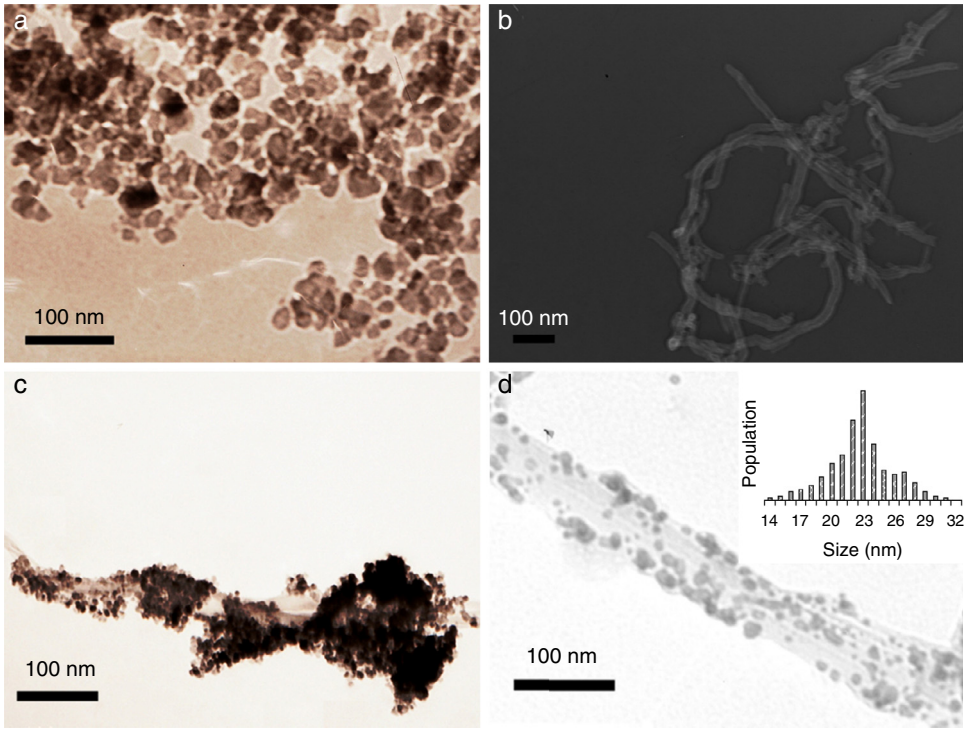

Fig. 4 – TEM images of (a) as prepared TiO_2 NPs, (b) purified CNT prepared through electrical arc discharge in DI water and (c) CNT–TiO_2 NPs coupled via simple mixing method and (d) magnified TEM image of CNT–TiO_2 NPs coupled via simple mixing method and the corresponding size distribution.

Ti—O—C bonds which causes reduction of band gap energy for photogenerating of electrons and holes. The IR absorption at 3400 cm^{-1} also arises from the superposition of the OH mode of interacting hydroxyl groups and symmetric and anti-symmetric OH modes of molecular water coordinated to Ti^{4+} cations [28,31].

3.3. *Microscopic studies*

The shape and size distribution of produced nanostructures were characterized by both SEM and TEM analyses. Fig. 3a–c shows SEM images of bare TiO_2 NPs prepared via sol–gel, pure CNTs prepared by arc discharge at 80 A arc current and the CNT–TiO_2 nanocomposites prepared by simple mixing methods, respectively. The results reveal that nearly spherical TiO_2 NPs with an appropriate size distribution are formed during the sol–gel process. Furthermore, Fig. 3b clearly reveals formation of high quality CNTs by arc discharge method after purification process. Moreover, it was found that TiO_2 NPs are well decorated on CNTs surface through simple mixing method. These results show that it is possible to easily decorate CNTs with TiO_2 NPs by simple mixing.

As clarified by SEM analysis CNTs with average diameter of ~50 nm were obtained in purified samples. TEM analysis provides more insight into the specific details of nanostructures due to the higher resolution. Fig. 4a–c demonstrates TEM images of bare TiO_2 NPs prepared via sol–gel, pure CNTs prepared by arc discharge at 80 A arc current and the CNT–TiO_2 nanocomposites prepared by simple mixing method, respectively. TEM images of the CNT–TiO_2 samples show the existence of well spread TiO_2 NPs, with almost narrow size distribution, along the tube walls of the samples (see Fig. 4d). In all three different coupling approaches, TiO_2 NPs were well decorated on the surface of CNTs and there was not any remarkable difference in the corresponding TEM images and therefore one of them is presented.

These results confirm that in all three coupling alternatives TiO_2 NPs attach to the CNT surface and form CNT–TiO_2 nanocomposites. But as we reported in details in our previous work the type of bonding is physisorption and TiO_2 NPs may detach from the CNT surface through some severe mechanical process such as sonication [10]. This implies that TiO_2 NPs may attach to the CNTs surface through van der Waals interactions.

3.4. *Photocatalytic activity measurements*

Fig. 5 illustrates the final kinetic curves of changes in Rh. B concentration under visible-light illumination for the CNT–TiO_2 nanocomposites through three different coupling alternatives. As is clear from the results the reaction rate changes are linear, which indicates that the photocatalytic reactions on CNT–TiO_2 surface can be expressed by the Langmuir–Hinshelwood model. The reaction rate after the adsorption equilibrium can be expressed as

$$-\mathrm{Ln}\left(\frac{C}{C_0}\right) = Kt$$

where C and C_0 are the reactant concentration at time $t = t$ and $t = 0$, respectively, K and t are the apparent reaction rate constant and time, respectively. In comparison with the

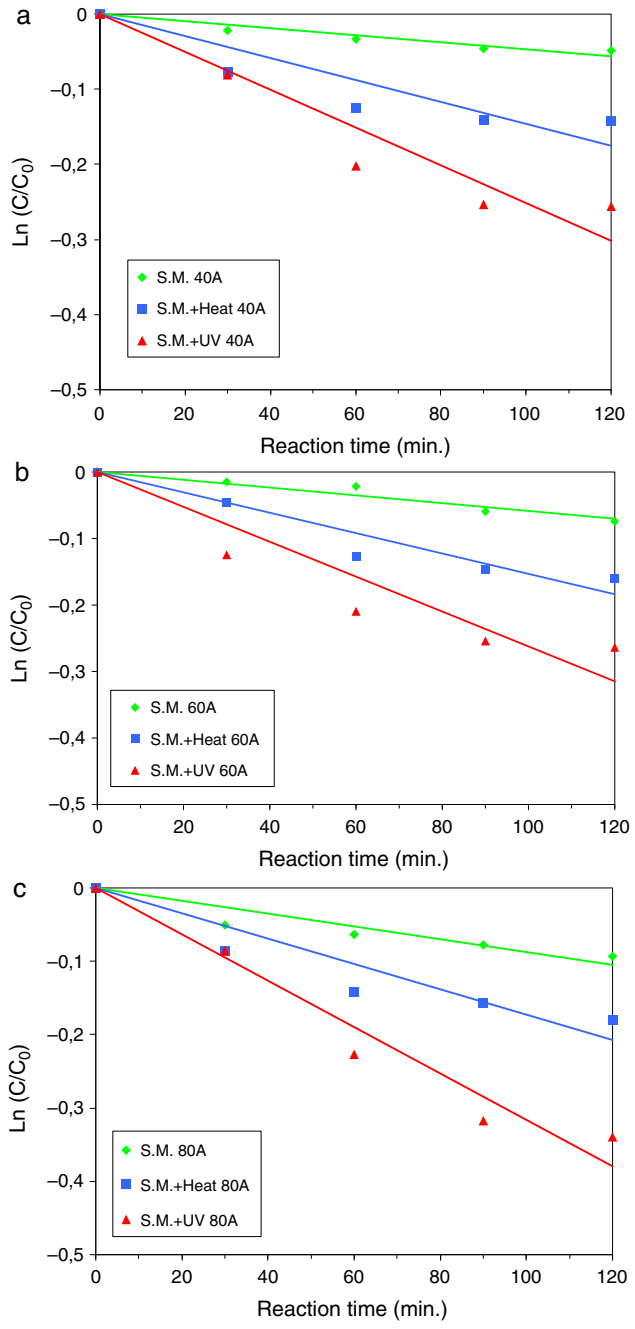

Fig. 5 – Changes in Rh. B concentration under visible-light illumination for CNT–TiO_2 nanocomposites prepared at different coupling alternatives.

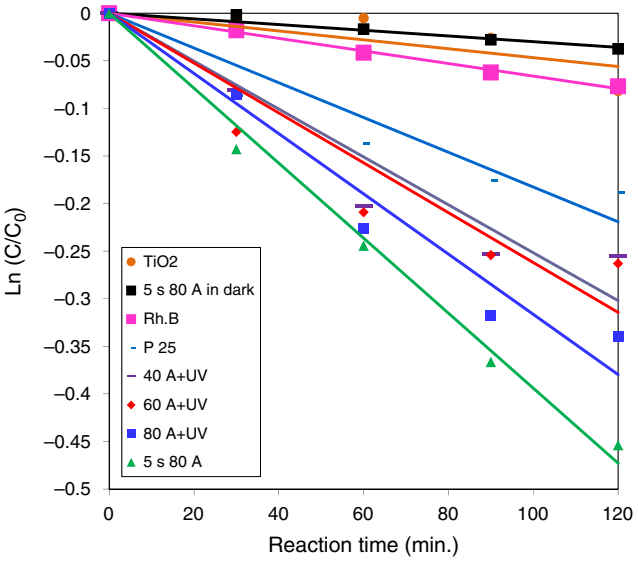

Fig. 6 – Comparison of the photocatalytic performance of CNT–TiO_2 nanocomposites with maximized reaction rate constants, pure TiO_2, blank Rh. B as a control and a commercial TiO_2 photocatalyst (Degussa P25).

Table 1 – Summary of the reaction rate constants of CNT–TiO_2 nanocomposites prepared by different methods.

Coupling method	Arc current (A)		
	40	60	80
	Reaction rate constant × 10^{-4} (min^{-1})		
Simple mixing	5	6	9
Simple mixing + heat treatment	15	15	17
Simple mixing + UV illumination	25	26	32

samples prepared by the same currents and different methods, UV illumination method had more influence on photocatalytic activity. Also by comparing Fig. 5a–c we observe that in each coupling method, 80 A sample has had the most influence on photocatalytic activity. So 80 A sample prepared via UV illumination method showed the highest photocatalytic yield among purified samples.

Fig. 6 demonstrates changes of Rh. B concentration under visible-light illumination for the samples with the best photocatalytic performance, pure TiO_2, blank Rh. B as a control and a commercial TiO_2 photocatalyst (Degussa P25) for comparison. As is clear from the results the sample prepared at 80 A arc current and 5 s arc duration has had the most photocatalytic activity among all samples. A summary of the reaction rate constants of CNT–TiO_2 nanocomposites prepared through the mentioned coupling methods is presented in Table 1. Also, a similar photocatalytic behavior and reaction rate constants of all mentioned samples were observed under UV light illumination and since the main objective of this study was the photocatalytic performance under visible-light irradiation, those data are not shown here.

4. Conclusion

CNT–TiO_2 nanocomposites were prepared using three different coupling protocols. XRD analysis revealed the formation of both CNT and TiO_2 phases and co-existence of them in composites. Furthermore, microscopic studies confirmed that the prepared TiO_2 NPs deposited onto the CNTs surface in all three different coupling alternatives. Photocatalytic performance of the CNT–TiO_2 nanostructures for decolorization of

Rh. B under visible-light irradiation showed that CNT incorporated into TiO_2 matrix, improved the photocatalytic efficiency under visible-light irradiation. It was found that samples prepared at 80 A under UV illumination method have had the best photocatalytic activity compared with simple mixed and heat treated CNT and TiO_2 samples. In fact introducing CNT into TiO_2 matrix facilitates longer charge separation by trapping photogenerated electrons and thus higher photocatalytic activity under visible-light irradiation.

Conflicts of interest

The authors declare no conflicts of interest.

Acknowledgment

This work was supported by Iran National Science Foundation (INSF).

REFERENCES

[1] Santangelo S, Faggio G, Messina G, Fazio E, Neri F, Neri G. On the hydrogen sensing mechanism of Pt/TiO_2/CNTs based devices. Sens Actuators B 2013;178:473–84.
[2] Tachikawa T, Majima T. Single-molecule, single-particle fluorescence imaging of TiO_2-based photocatalytic reactions. Chem Soc Rev 2010;39:4802–19.
[3] Habisreutinger SN, Schmidt-Mende L, Stolarczyk JK. Photocatalytic reduction of CO_2 on TiO_2 and other semiconductors. Angew Chem Int Ed 2013;52:7372–408.
[4] Wilson D, Wang W, Lopes RJG. Ceria-doped and TiO_2 nanocomposite coating on multiwalled carbon nanotubes for the photocatalytic remediation of agro-industrial wastewaters. Appl Catal B 2012;123–124:273–81.
[5] Akhavan O. Lasting antibacterial activities of Ag–TiO_2/Ag/a–TiO_2 nanocomposite thin film photocatalysts under solar light irradiation. J Colloid Interface Sci 2009;336:117–24.
[6] Akhavan O, Abdolahad M, Abdi Y, Mohajerzadeh S. Synthesis of titania/carbon nanotube heterojunction arrays for photoinactivation of *E. coli* in visible light irradiation. Carbon 2009;47:3280–7.
[7] Ashkarran AA, Kavianipour M, Aghigh SM, Afshar SAA, Saviz S, Zad AI. On the formation of TiO_2 nanoparticles via submerged arc discharge technique: synthesis, characterization and photocatalytic properties. J Cluster Sci 2010;21:753–66.
[8] Akhavan O, Azimirad R. Photocatalytic property of Fe_2O_3 nanograin chains coated by TiO_2 nanolayer in visible light irradiation. Appl Catal A 2009;369:77–82.
[9] Ashkarran AA, Aghigh SM, Kavianipour M, Farahani NJ. Visible light photo- and bioactivity of Ag/TiO_2 nanocomposite with various silver contents. Curr Appl Phys 2011;11:1048–55.
[10] Ashkarran AA, Fakhari M, Mahmoudi M. Synthesis of a solar photo and bioactive CNT–TiO_2 nanocatalyst. RSC Adv 2013;3:18529–36.
[11] Elias CN, Meyers MA, Valiev RZ, Monteiro SN. Ultrafine grained titanium for biomedical applications: an overview of performance. J Mater Res Technol 2013;2:340–50.
[12] Ghorai TK, Biswas N. Photodegradation of rhodamine 6G in aqueous solution via $SrCrO_4$ and TiO_2 nano-sphere mixed oxides. J Mater Res Technol 2013;2:10–7.
[13] Li Z, Gao B, Chen GZ, Mokaya R, Sotiropoulos S, Li PG. Carbon nanotube/titanium dioxide (CNT/TiO_2) core–shell nanocomposites with tailored shell thickness, CNT content and photocatalytic/photoelectrocatalytic properties. Appl Catal B 2011;110:50–7.
[14] Bouazza N, Ouzzine M, Lillo-Ródenas MA, Eder D, Linares-Solano A. TiO_2 nanotubes and CNT–TiO_2 hybrid materials for the photocatalytic oxidation of propene at low concentration. Appl Catal B 2009;92:377–83.
[15] Chekin F, Bagheri S, Abd Hamid SB. Synthesis of Pt doped TiO_2 nanoparticles: characterization and application for electrocatalytic oxidation of l-methionine. Sens Actuators B 2013;177:898–903.
[16] Cong Y, Zhang J, Chen F, Anpo M. Synthesis and characterization of nitrogen-doped TiO_2 nanophotocatalyst with high visible light activity. J Phys Chem C 2007;111:6976–82.
[17] Cong Y, Zhang J, Chen F, Anpo M, He D. Preparation, photocatalytic activity, and mechanism of nano-TiO_2 Co-doped with nitrogen and iron (III). J Phys Chem C 2007;111:10618–23.
[18] Elahifard MR, Rahimnejad S, Haghighi S, Gholami MR. Apatite-coated Ag/AgBr/TiO_2 visible-light photocatalyst for destruction of bacteria. J Am Chem Soc 2007;129:9552–3.
[19] Hu C, Lan Y, Qu J, Hu X, Wang A. Ag/AgBr/TiO_2 visible light photocatalyst for destruction of azodyes and bacteria. J Phys Chem B 2006;110:4066–72.
[20] Jagadale TC, Takale SP, Sonawane RS, Joshi HM, Patil SI, Kale BB, et al. N-doped TiO_2 nanoparticle based visible light photocatalyst by modified peroxide sol–gel method. J Phys Chem C 2008;112:14595–602.
[21] Lu J, Su F, Huang Z, Zhang C, Liu Y, Ma X, et al. N-doped Ag/TiO_2 hollow spheres for highly efficient photocatalysis under visible-light irradiation. RSC Adv 2013;3:720–4.
[22] Marikkannan SK, Ayyasamy EP. Synthesis, characterisation and sintering behaviour influencing the mechanical, thermal and physical properties of cordierite-doped TiO_2. J Mater Res Technol 2013;2:269–75.
[23] Sedneva TA, Lokshin EP, Belikov ML. Ferroin adsorption on TiO_2-based photocatalytic materials. Inorg Mater 2012;48:480–7.
[24] Kingston CT, Simard B. Fabrication of carbon nanotubes. Anal Lett 2003;36:3119–45.
[25] Lim SH, Luo Z, Shen Z, Lin J. Plasma-assisted synthesis of carbon nanotubes. Nanoscale Res Lett 2010;5:1377–86.
[26] MacKenzie KJ, Dunens OM, See CH, Harris AT. Large-scale carbon nanotube synthesis. Recent Patents Nanotechnol 2008;2:25–40.
[27] Ashkarran AA. Metal and metal oxide nanostructures prepared by electrical arc discharge method in liquids. J Cluster Sci 2011;22:233–66.
[28] Maira AJ, Coronado JM, Augugliaro V, Yeung KL, Conesa JC, Soria J. Fourier transform infrared study of the performance of nanostructured TiO_2 particles for the photocatalytic oxidation of gaseous toluene. J Catal 2001;202:413–20.
[29] Woan K, Pyrgiotakis G, Sigmund W. Photocatalytic carbon-nanotube–TiO_2 composites. Adv Mater 2009;21:2233–9.
[30] Cooke DJ, Eder D, Elliott JA. Role of benzyl alcohol in controlling the growth of TiO_2 on carbon nanotubes. J Phys Chem C 2010;114:2462–70.
[31] Maira AJ, Yeung KL, Lee CY, Yue PL, Chan CK. Size effects in gas-phase photo-oxidation of trichloroethylene using nanometer-sized TiO_2 catalysts. J Catal 2000;192:185–96.